

Transition to Turbulence in Pipe Flow

T. Mullin and J. Peixinho

*School of Physics and Astronomy, The University of Manchester, Oxford Road, Manchester
M13 9PL, UK
E-mail: tom.mullin@mau.ac.uk*

We review the results of recent experimental investigations into transition to turbulence in fluid flow through a circular straight pipe, at room temperature. The stability of Hagen–Poiseuille flow was investigated using impulsive perturbations by either injecting or sucking small amounts of fluid through holes in the wall of the pipe. The evolution of the induced patches of disturbed flow were observed using flow visualization and laser Doppler velocimetry. The principle result obtained was a finite amplitude stability curve where the critical amplitude of the disturbance required to cause transition is found to be inversely proportional to the Reynolds number. Estimates for the lower threshold value of Reynolds number which is required to sustain turbulence were also measured.

1. INTRODUCTION

The onset of turbulence in the flow through a long circular straight pipe has intrigued scientists since Reynolds' experimental investigations¹ at the end of the 19th century. The problem is simple in concept and yet the origins of the observed turbulent motion remain largely mysterious despite more than a century of research. The principle issue is that all theoretical and numerical work suggests that the flow is linearly stable,^{2,3} i.e. it remains laminar for all Re and yet most practical pipe flows are turbulent. Hence, there is a direct conflict between theory and observation (here $Re = UD/\nu$, where U is the mean velocity, D the pipe diameter and ν is the kinematic viscosity of the fluid).

Reynolds found the onset of what he called “sinuous” flow depends on the nondimensionalized flow rate and this parameter is now called the Reynolds number. He observed that in uncontrolled experiments turbulence appeared naturally at $Re \approx 2000$ and was triggered by inlet disturbances to the pipe. However, Reynolds also noted that the laminar state

could be maintained to $Re \approx 13,000$ if he took great care in minimizing external disturbances to the flow. A clear example of the effects of controlling background effects is provided by Pfenninger⁴ who managed to obtain laminar flows up to $Re \approx 100,000$ by taking extraordinary care. Studies of transition to turbulence in pipe flows using cryogenic fluids are rare although the results of an extensive experimental investigation of turbulent pipe flow using liquid helium has been reported.⁵ Some results are also reported for transition to turbulence and they are consistent with those obtained using conventional fluids.

All experimental evidence suggests that transition to turbulence in pipe flow is finite amplitude in nature. Experimental results have been reported for a finite amplitude threshold curve⁶ where transition to turbulence was found above a critical amplitude of perturbation and the amplitude exhibited systematic dependence on Re . The threshold is found to be probabilistic in nature with a narrow normal distribution where the mean is used to identify transition and the width provides an estimate of the errors. Darbyshire and Mullin's perturbation system⁶ involved injecting and subtracting a short pulse of fluid tangentially through a small number of holes equally spaced around the circumference of the pipe. A range of perturbations have been employed by other investigators including using a larger number of holes,^{7,8} continuous flow injected through a porous wall⁹ and periodic suction and injection.^{10,11} The general consensus is that there is some sensitivity of Hagen–Poiseuille flow to the form and type of imposed perturbation but the specific part of the perturbation which is responsible for transition is yet to be identified. The qualitative features reported in the Darbyshire and Mullin investigation⁶ have also been observed in studies of the stability of a rotating sample of $^3\text{He-B}$.^{12,13} The transition to turbulence is subcritical so that a finite amplitude threshold for injected perturbations must be crossed before turbulence arises. As in pipe flow, the transition is probabilistic with a normal distribution of perturbation amplitudes close to the threshold boundary. A qualitative difference with transition in pipes is that the two final states of the flow are either vortex-free superflow or turbulence with discrete vortices, whereas they are either Poiseuille flow or sustained turbulence in pipes.

In a more recent investigation of pipe flow transition,¹⁴ a novel type of perturbation was used to reveal a scaling relationship for the amplitude of perturbation required to cause transition to turbulence as a function of Re . The novel feature was that it allowed for a separation of amplitude and timescales of the perturbation by injecting a boxcar distribution of perturbed fluid into the main flow field. It was firmly established that the important criterion was the length of the flow field which was perturbed

and this enabled the uncovering of a $O(Re^{-1})$ scaling law for the amplitude of perturbation required to cause transition over the range $2000 < Re < 20,000$. This is found to be true provided the initial perturbation disturbed more than 10 pipe diameters of the flow. Some evidence for such scaling laws has been reported previously for pipe flows,⁹ boundary layers,¹⁵ and they have also been found for plane Couette flows.¹⁶ One surprising consequence of the scaling law for pipe flows is that the absolute amplitude of the perturbation remains relatively large with increasing Re . Therefore, theories based on local analyses of the trivial state may not provide much insight into transition since the basin of attraction of the laminar state remains finite even at modest Re . This appears to contradict many observations which show that very small amplitude disturbances are required to promote turbulence at high Re . However, it was shown by Reynolds and many others subsequently that the inlet flow is very sensitive to perturbations so that fully developed Poiseuille flow is evidently more robust. Moreover developing flow is known to be linearly unstable¹⁷ albeit at values of $Re \approx 10,000$.

Clearly the Re^{-1} scaling law cannot hold for small Reynolds numbers where all previous results indicate that the flow is globally stable. This apparent contradiction was resolved recently¹⁸ where it was shown that when $Re \leq 1760$, impulsive small amplitude perturbations introduced into fully developed Hagen–Poiseuille flow decayed as they traveled downstream, i.e. when $Re \leq 1760$ all perturbations decay and turbulent flow cannot be maintained. On the other hand, for $Re \geq 1760$, perturbations of sufficient amplitude give rise to transition to the nontrivial state of turbulence. At these values of Re the turbulence is localized and has the form of an “equilibrium turbulent puff.”¹⁹ A sequence of flow visualization photographs of a typical puff at $Re = 2300$ is shown in Fig. 1. Puffs are ~ 20 diameters long and travel at $\sim 0.9U$ and hence the mean flow passes through the sharp rear interface of the puff. They maintain their form as they travel along the pipe with rear half of highly disordered flow with a weak decaying wave at the front. When $Re \geq 3000$ the localized region of fluid formed on transition contains fully disordered motion and both front and rear interfaces are sharp. The leading edge travels faster than the mean flow and the rear slower and hence the patch of disordered motion spreads as it travels. These blocks of disordered motion are now referred to as slugs.¹⁹ The motion inside the patch is not fully turbulent and flows with the statistical properties of fully developed turbulence are not found until $Re \geq 5000$. Transition at even greater values of Re is abrupt and rapidly fills the pipe. Modern numerical computations of some specific perturbations applied to Hagen–Poiseuille flow have also produced

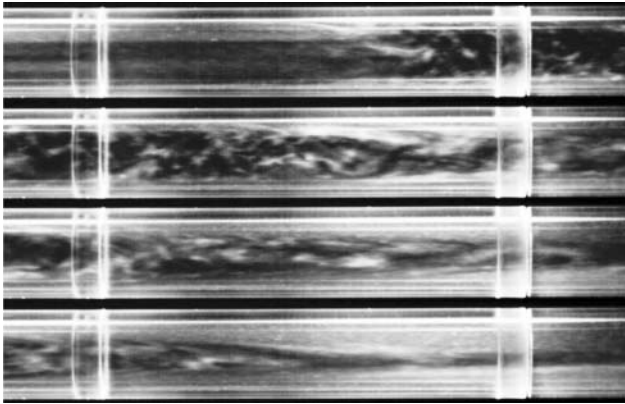


Fig. 1. Flow visualization of an equilibrium puff at $Re=2300$. The mean flow U is 11.5 cm/second. Each photograph is taken at a fix location at 1 second time intervals. Flow is from left to right and the first photograph in the sequence is at the bottom and the last at the top. The weak wave at the front of the puff can just be discerned in the middle of the bottom photograph and the sharp rear interface in the middle of the top picture.

puffs^{20,21} and computational approaches can now reproduce the structures seen in experiments.

Here, we review results of recent investigations into transition to turbulence in pipe flows. We begin by highlighting the sequence of events close to the threshold boundary where the rapid nonlinear development of sustained turbulence is identified in a new flow visualization investigation. In the second investigation, the lifetimes of the puff states found at low Re are studied in terms of the statistics of the evolution of controlled perturbations. This has enabled us to uncover a sharp lower bound for the existence of sustained turbulence and complements the existing scaling law for the threshold amplitude law. It thus enables a more complete description of the boundary between laminar and turbulent flows in amplitude versus Re space.

2. EXPERIMENTAL DETAILS

A schematic diagram of the apparatus is presented in Fig. 2. The pipe had a diameter $D = 20 \pm 0.01$ mm and was constructed from 100, 150 mm long machined sections push-fitted together and butted flush so that there was no measurable gap between each section. This method of construction was used to ensure a long straight pipe which was circular to the machining accuracy of ± 0.02 mm. The pipe was held on a steel



Fig. 2. (Color on-line) Schematic of the constant mass flux pipe facility. The pipe, the reservoir, and the piston are up to scale. The temperature of the laboratory was controlled to $\pm 1^\circ\text{C}$ at a mean temperature of 20°C .

base and had a total length of 15 m ($750D$) and was aligned using a laser. A reservoir with a capacity of 100 l was connected to the pipe through a smooth trumpet shaped inlet. A 30 cm diameter stainless steel piston was mounted on hardened fibre piston rings inside a ground steel cylinder and this pulled the fluid at a constant mass flux along the pipe using a computer controlled motor and lead screw arrangement. Hence, even if the motion became turbulent, the mass flux through the pipe was unaffected so that the Re remained constant. The long-term temperature stability of the laboratory was controlled to $\pm 1^\circ\text{C}$ at a mean temperature of 20°C . A typical temperature gradient recorded from several thermocouple along the pipe was 0.2°C . By these means, we were able to maintain an accuracy in Re of better than 1%. The facility enabled a laminar flow to be achieved up to a flow rate corresponding to $Re = 23,000$. Laminar pipe flow could only be obtained at such high Re by allowing settling times of ~ 1 hour to ensure that disturbances in the header tank had decayed. This emphasizes the point that pipe flow is very sensitive to inlet disturbances but, once Poiseuille flow has developed, a finite amplitude perturbation is required to cause transition in practice. The experimental work here was performed by perturbing fully developed Poiseuille flow which is achieved in a length of $\sim Re/30$ (in diameters).²²

The flow state was monitored using Mearlmaid Pearlescence as flow visualization and a vertical thin sheet of light was used to illuminate the flow across a diameter of the pipe. Observations were made in a direction orthogonal to the lightsheet and this technique was used to produce Fig. 1 and the other photographs used here. Single point velocity measurements were made using a laser Doppler velocimeter in separate experiments. Velocity profiles are presented in Fig. 3. The mean velocity profiles obtained in laminar flows are in very good agreement with the well known parabolic velocity distributions with $u = 2U$ where u is the maximum centreline speed and U is the mean. The mean velocity profile in turbulent flow obtained at $Re = 5300$ is also in good agreement with previous measurements (i.e. Ref. 23).

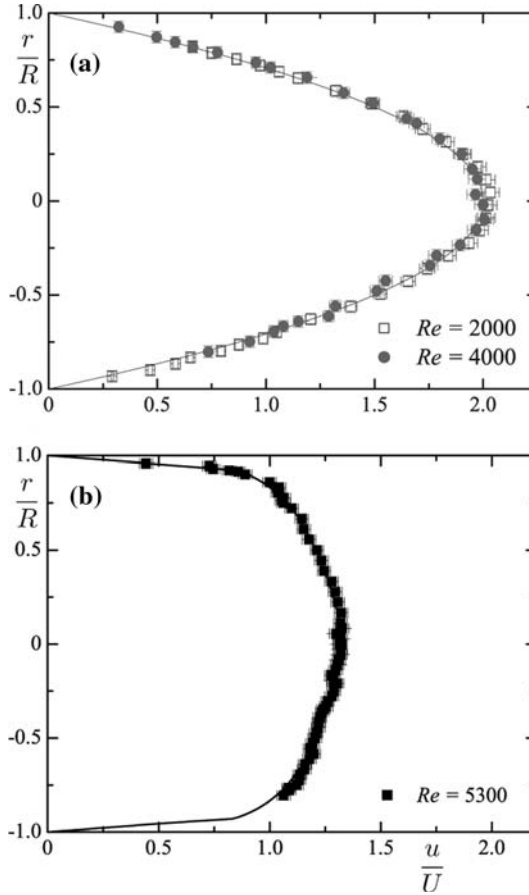


Fig. 3. (a) Velocity profiles measured in laminar flows at $Re=2000$ and 4000 . The solid line corresponds a parabolic profile. (b) A mean velocity profile measured in a turbulent flow a $Re=5300$ (the lines correspond to a linear and log fit).

3. RESULTS AND DISCUSSION

3.1. Evolution of Disturbances

Hof *et al.*¹⁴ developed an injection system which permits the amplitude and width of the perturbation to be varied independently. In essence, the disturbance is a pulse of fluid which is injected through a set of six small holes arranged azimuthally around the pipe. The pulse or boxcar has a width Δt and a nondimensional amplitude A which is the ratio of the amount of fluid injected to the mean mass flux of the pipe. For $Re \geq 2000$

and at a given value of Δt , there is a threshold amplitude A_c above which transition to turbulence takes place. The disturbance is advected along by the mean flow and hence the initial width of the disturbed region is proportional to Re . Observation suggests that this is a key parameter in the transition process. Specifically, provided that more than $10D$ of the flow is disturbed, the threshold amplitude of the perturbation is found to be independent of Re . In fact, the response curve obtained over the entire range of lengths of perturbation widths can simply be scaled by Re .¹⁴

In the present experiments, we have used the same approach but first report results using a single jet to simplify the evolution procedure. A boxcar disturbance was introduced into a fully developed Hagen–Poiseuille flow 185 diameters from the pipe entrance at $Re = 2000$ through a single hole. The injected volume flux was controlled to within 10^{-2} ml/second and a video camera travelling at the mean flow velocity in the pipe recorded images of the development of the disturbances. In general, for a relatively small amplitude, the disturbances decayed as they progressed downstream. For amplitudes close to the threshold, the disturbances were initially amplified but then decayed with increasing distance downstream. At higher amplitudes, transition to a patch of sustained disordered motion occurred and the flow contained an “equilibrium turbulent puff.”¹⁹ Two typical sequences, one obtained just below the threshold for transition and the other just above it are shown in Fig. 4. The development of a decaying disturbance can be seen in Fig. 4(a)–(f) and the relatively rapid development of a puff is shown in Fig. 4(g)–(l).

The principle features associated with the decaying disturbance (Fig. 4(a)–(f)) are the spread of the jet within the flow (Fig. 4(a)–(c)) and the development of well-defined flow structures (Fig. 4(b)–(c)). Further downstream, the structures are simply advected (Fig. 4(d) and (e)) along by the mean flow up to ~ 14 diameters from the point of injection. In practice, experience shows that decay of the perturbation has already started at six diameters (D) before approximately unidirectional flow is recovered at 30 diameters (Fig. 4(f)).

In the case of a jet disturbance which triggers a puff (Fig. 4(g)–(l)), the jet again spreads within the flow and structures are again created across the flow field (Fig. 4(h)) which are similar in form to those seen in the decaying case (Fig. 4(b)). However, the subsequent sequence, Fig. 4(i) and (j), show the rapid creation of a puff where we only illustrate the trailing edge features here. Further downstream, (Fig. 4(k) and (l)), breakdown to turbulence takes place so that disordered motion covers almost the entire field of view.

We now consider the effect of a disturbance which has the form of a short boxcar of suction. Again a threshold was found and we illustrate

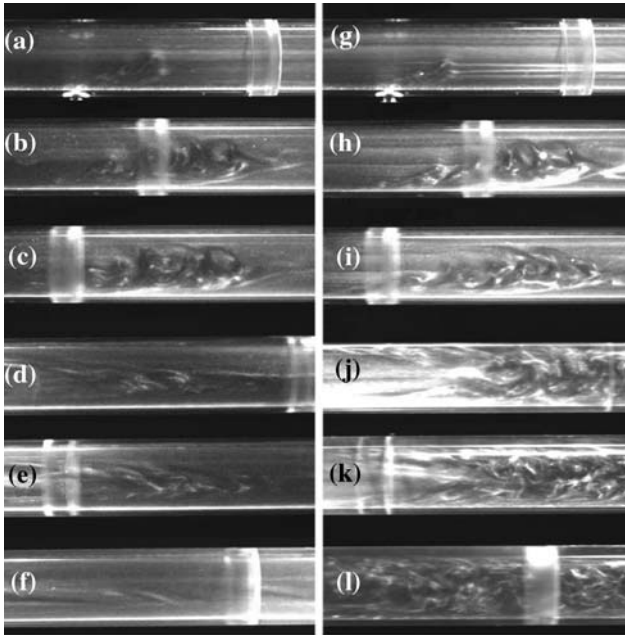


Fig. 4. Development of a perturbation where a small amount of fluid was impulsively injected into the bulk flow through a 3 mm hole. $Re = 2000$ and in the snapshot sequence (a)–(f) the perturbation decays. Images taken at 1, 2, 3, 6, 14 and 30 diameters downstream from the injection point using a camera travelling at the mean speed of the flow. In the sequence (g)–(l) a slightly larger amount of fluid was injected and a puff is created.

typical evolution sequences on either side of the boundary by the sets of photographs given in Fig. 5. It is interesting to note the levels of flux used now are typically two orders of magnitude larger than for the case of injection. This significantly larger perturbation means that obtaining a full threshold curve as a function of Re was not possible. Instead, we include the flow visualization results here to compare and contrast with the processes involved in transition created by injection. The immediate difference which can be seen in Fig. 5(a) and (g) is a large distortion of the flow field immediately after the perturbation has been applied instead of a jet. Eddies are then formed close to the boundary (Fig. 5(b) and (h)) and these grow to create disturbances away from the wall in both cases Fig. 5(c) and (d) and (i)–(k). However, decay of the disturbed flow field is then evident in Fig. 5(e) and (f) whereas the rapid nonlinear development of a puff can be seen in Fig. 5(k) and (l).

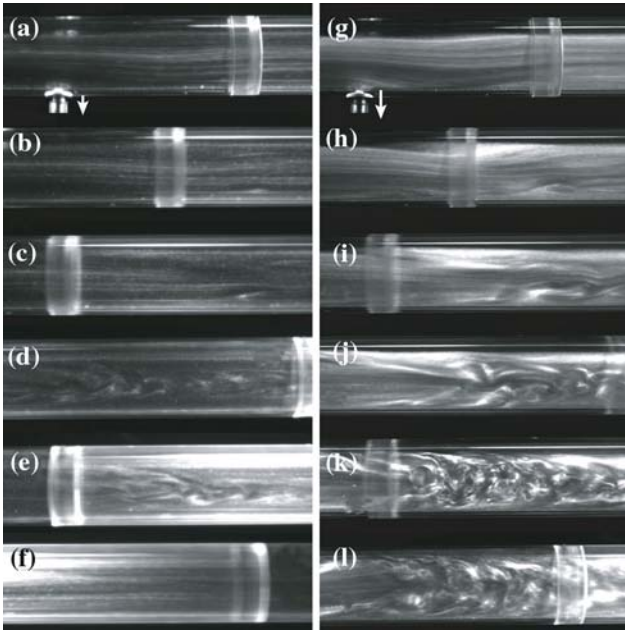


Fig. 5. Development of a perturbation where a amount of fluid was impulsively sucked through a 3 mm hole. $Re = 2000$ and in the sequence (a)–(f) the perturbation decays. Images taken at 1, 2, 3, 6, 14 and 30 diameters downstream from the perturbation point. In the sequence (g)–(l) a slightly larger amount of fluid was extracted and a puff is created.

3.2. Decay of Injected Disturbances

All previous investigations have indicated that the flow is globally stable for $Re \leq 2000$ although precise values of this estimate have only recently been established¹⁸. Hence all disturbances created in the flow field below this value will decay since turbulent motion cannot be sustained. The present investigation was carried out to test this hypothesis by injecting large amplitude well defined perturbations into fully developed Hagen–Poiseuille flow and observing their development as they progressed downstream. Here, the perturbation was created using a boxcar pulse of fluid which was injected tangential to the main flow via a ring of six equally spaced 0.5 mm holes. Observations were made using flow visualization and a travelling video camera which recorded images of the patch of disordered fluid as it traveled along. Several light boxes were suspended above the pipe and provided a light sheet along its length. The lights were switched on and off sequentially to avoid heating effects. In the first $100D$ the perturbation evolved in a complicated way similar to

those described above. After this initial transient phase the disturbed flow was observed to be localized and traveled along close to the mean speed of the flow. The values of Re investigated were such that the final state far downstream was, typically, laminar flow. Image analysis of the video recording permitted estimates to be made of the positions at which disturbed motion decayed (measured in diameters D from the location of perturbation input). The initial stage of the decay was subtle but the final collapse was clear since a rapid return to featureless flow was observed.

The results presented in Fig. 6(a) and (c) are plots of the probability of observing a localized disturbed region of flow, plotted as a function of distance downstream in D from the point of injection of the perturbation which corresponds to zero on the abscissa. The downstream limit was set by the length of the pipe at $500D$ from the perturbation input location. This was not a severe limitation in practice since very few decaying disturbances survived to this station. The initial conditions for the perturbation were such that they were all $10D$ long and the amplitudes used in Fig. 6(a) and (b) and (b) and (c) were $A = 0.1$ and $A = 0.01$, respectively. Between 40 and 100 independent experimental runs were performed for each value of Re in order to obtain good statistical estimates for the distance of propagation. The straight lines correspond to least squares fits of exponentials such that $P(D) \propto \exp(-\epsilon D)$, where ϵ is the rate of decay of the disturbed state. The quality of the fits indicate that the disturbed flow decays exponentially to a good approximation²⁴. It can be seen in Fig. 6(a) and (b) that the slopes are significantly steeper for smaller values of Re , i.e. there is faster decay at lower Re . This behaviour is expected and is consistent with observations by Bottin and Chat e²⁵ for experiments on plane Couette flow and Faisst and Eckhardt²⁶ for a model pipe flow.

A useful measure that can be extracted from the exponential fits is time required for half the initial states to decay which is defined as $\tau = (\ln 2)/\epsilon$. We will refer to this as the ‘‘half-life’’ of a perturbation. Graphs of the half life of the disturbed flow for the two perturbation amplitudes $A = 0.1$ and $A = 0.01$ are shown plotted as a function of Re in Fig. 6(b) and (d) where a divergence in the timescales is evident. Plots of the inverse of half-life τ^{-1} versus Re are shown in the respective insets of Fig. 6(b) and (d). It may be seen that τ^{-1} passes through zero at 1695 ± 20 and 1820 ± 20 , respectively. At these critical values of Re the half-life τ approaches infinity and the perturbation does not decay but develops into a turbulent puff which persists. Hence this gives a method for estimating the threshold for transition to turbulence at low Re . The estimate is consistent with the recent value of $Re = 1760$ obtained by observing the decay

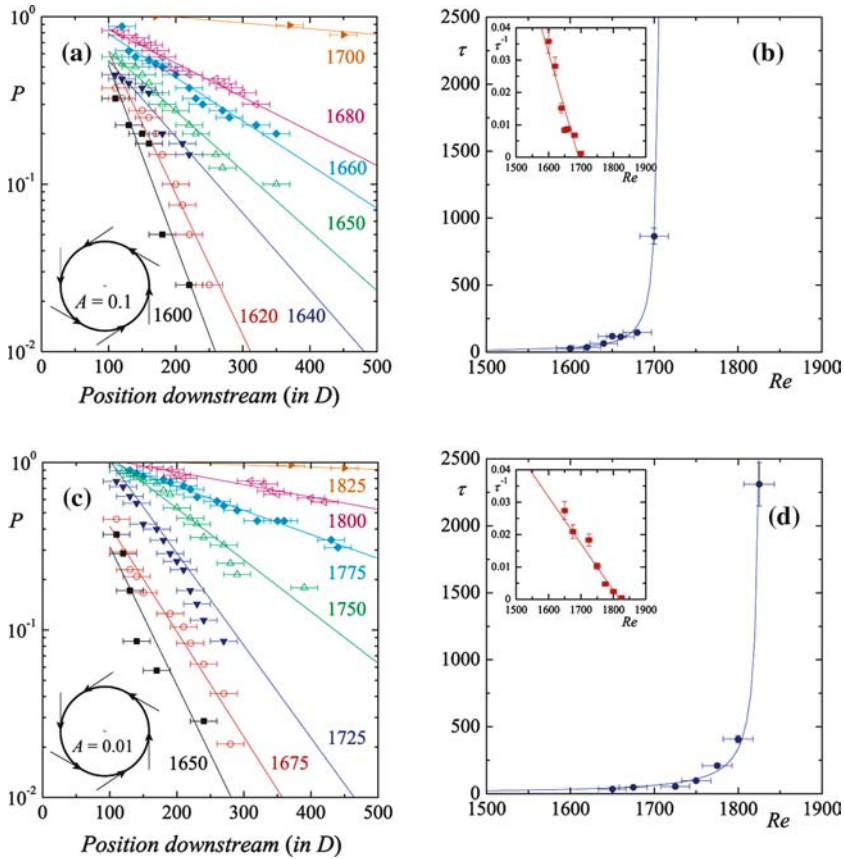


Fig. 6. (Color on-line) Turbulent lifetimes for different transitional Reynolds numbers for two different amplitudes: $A = 0.1$ and $A = 0.01$. (a) Probability P for a single run to still be turbulent after a distance D for seven Reynolds numbers as indicated. Between 50 and 100 experimental runs been evaluated per Reynolds number. The distributions are described well by exponential distributions shown as straight lines. (b) Half-life τ of the turbulent lifetimes as a function of Re . The error bars indicate the uncertainty in the measurements. The inset shows the inverse half-life versus Re and a linear fit, corresponding to a law $\tau(Re) \propto (Re_c - Re)^{-1}$, with $Re_c \approx 1695$ and 1820 , respectively, for $A = 0.1$ and $A = 0.01$.

of turbulence by reducing Re .¹⁸ This agreement is encouraging and points to a robustness of this lower bound since the present experiment involves the injection of relatively large amplitude perturbations which have an unknown effect on the mean flow whereas the earlier work¹⁸ is concerned with the decay of a “natural” state of the system, a turbulent puff.

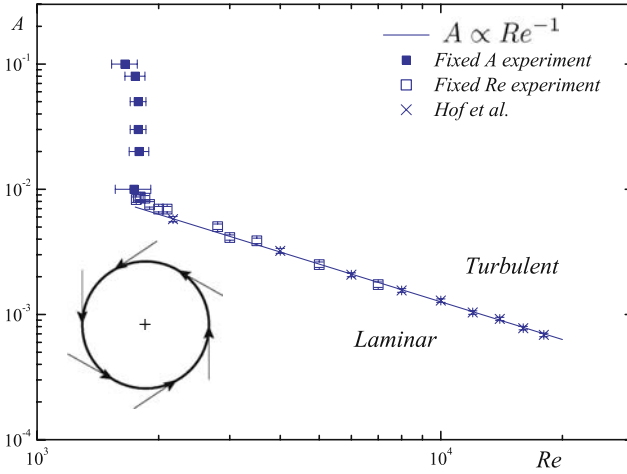


Fig. 7. (Color on-line) Finite amplitude threshold curve A versus Re . The amplitude A of the perturbation is made nondimensional by dividing by the mass flux of the main flow. The lower bound was estimated by measuring a divergence in time-scales in the decay of injected perturbations. The Re^{-1} was found by increasing the amplitude of the perturbation at fixed Re .

3.3. Finite Amplitude Stability Curve

As discussed above, when an injection system is used which permits the amplitude and width of the perturbation to be varied independently, the transition threshold is fixed for any given value of Re provided the initial disturbance affects a length $\geq 10D$ of the flow. This enabled the uncovering of a scaling law which indicates that the amplitude of perturbation required to cause transition scales as $O(Re^{-1})$ for $2000 \leq Re \leq 20,000$. An interpretation of this result is that it reflects the balance between viscous and inertia terms in the Navier Stokes equations.

We have added to these results and a compilation of both sets of results is presented in Fig. 7. These results were obtained at fixed values of Re and increasing the amplitude of the perturbation until transition was observed. As discussed above, this is a probabilistic process so that on average 40 runs of the experiment had to be performed for each value of Re . Reliable estimates of the threshold were obtained and there is very good agreement between these new observation and the previous results so that a $O(Re^{-1})$ scaling law is confirmed. It is interesting to note that the same scaling law has also been found recently for a single jet²⁷. The estimates for the lower bound for sustained turbulence have been added to the scaling law data in Fig. 7. Hence there is now a clear demarcation in

(A, Re) space between regions where laminar flow persists and turbulent or disordered flow is possible.

4. CONCLUSION

The results presented here are in accord with theory in that they support that notion that the transition threshold in a circular pipe is finite amplitude in nature. Despite the obvious experimental difficulties such as deciding on the exact nature of the amplitude and form of any imposed “perturbation”, a definite scaling law for the threshold for transition has been uncovered. Moreover, a reliable estimate for the lower bound for sustained turbulent motion has been obtained. Qualitative similarities with recent work in rotating ${}^3\text{He-B}^{12,13}$ are intriguing and it remains to be seen if this overlap can be developed further.

ACKNOWLEDGMENTS

We thank M. Krusius for helpful comments on an earlier draft of this paper. The authors are grateful to EPSRC for funding this research. TM is supported by a ‘Senior Fellowship’ and JP by the research grant GR/576137/01.

REFERENCES

1. O. Reynolds, *Proc. R. Soc. A* **35**, 88 (1883).
2. P. G. Drazin and W. H. Reid, *Hydrodynamic Stability*, Cambridge University Press (1980).
3. Y. Pomeau, *Physica D* **23**, 3 (1986).
4. W. Pfenniger, in *Boundary Layer and Flow Control*, G. V. Lachman (ed.), Pergamon (1961).
5. C. J. Swanson, B. Julian, G. G. Ihas, and R. J. Donnelly, *J. Fluid Mech.* **461**, 51 (2002).
6. A. G. Darbyshire and T. Mullin, *J. Fluid Mech.* **289**, 83 (1995).
7. L. Bergström, *Eur. J. Mech., B/Fluids*, **12**, 749 (1993).
8. L. Bergström, *Eur. J. Mech., B/Fluids*, **14**, 601 (1995).
9. A. A. Draad, G. D. C. Kuiken, and F. T. M. Nieuwstadt, *J. Fluid Mech.* **377**, 267 (1998).
10. S. Eliahou, A. Tumin, and I. Wygnanski, *J. Fluid Mech.* **361**, 333 (1998).
11. G. Han, A. Tumin, and I. J. Wygnanski, *J. Fluid Mech.* **419**, 1 (2000).
12. A. P. Finne, T. Araki, R. Blaauwgeers, V. B. Eltsov, N. B. Kopnin, M. Krusius, L. Skrebek, M. Tsubota, and G. E. Volovik, *Nature* **424**, 1022 (2003).
13. A. P. Finne, S. Boldarev, V. B. Eltsov, and M. Krusius, *J. Low Temp. Phys.* **138**, 567 (2005).
14. B. Hof, A. Juel, and T. Mullin, *Phys. Rev. Lett.* **91**, 244502 (2003).
15. R. Govindarajan, and R. Narasimha, *J. Fluids Eng.* **113**, 147 (1991).
16. O. Dauchot and Daviaud, *Phys. Fluids* **7**, 335 (1995).
17. D. F. da Silva, and E. A. Moss, *J. Fluids Eng.* **116**, 61 (1994).
18. J. Peixinho, and T. Mullin, *Phys. Rev. Lett.* **96**, 094501 (2006)
19. I. J. Wygnanski, and F. H. Champagne, *J. Fluid Mech.* **59**, 281 (1973).

20. B. Ma, C. W. H. van Doorne, Z. Zhang, and F. T. M. Nieuwstadt, *J. Fluid Mech.* **398**, 181 (1999).
21. J. Reuter, and D. Rempfer, *Theor. Comput. Fluid Dyn.* **17**, 273 (2004).
22. D. J. Tritton, *Physical Fluid Dynamics*, Oxford University Press (1988).
23. V. C. Patel, and M. R. Head, *J. Fluid Mech.* **38**, 181 (1969).
24. K. R. Sreenivasan, *Acta Mech.* **44**, 1 (1982).
25. S. Bottin, and H. Chaté, *Eur. Phys. J. B* **6**, 143 (1998).
26. H. Faisst, and B. Eckhardt, *J. Fluid Mech.* **504**, 343 (2004).
27. B. Hof, in *Proceedings of the IUTAM Symposium Laminar–Turbulent Transition and Finite amplitude Solutions*, T. Mullin and R. R. Kerswell, (eds.), Springer (2005).